THE JOURNAL OF PHYSICAL CHEMISTRY B

ARTICLE

pubs.acs.org/JPCB

Physical Aging Enhanced Mesomorphic Structure in Melt-Quenched Poly(L-lactic acid)

Tongping Zhang, Jian Hu, Yongxin Duan,* Fuwei Pi, and Jianming Zhang*

Key Laboratory of Rubber-Plastics, Ministry of Education/Shandong Provincial Key Laboratory of Rubber-Plastics, Qingdao University of Science & Technology, Qingdao City 266042, People's Republic of China

ABSTRACT: The structural evolutions and kinetics of melt-quenched poly(L-lactic acid) (PLLA) during the process of isothermal physical aging below the glass transition temperature (T_g) were investigated by time-resolved infrared spectroscopy. The results show that local ordered structure is developed with aging time. Such local ordered structure shows the same characteristic band at 918 cm^{-1} as that of the mesomorphic structure formed during the unaxially drawn process of PLLA from the glassy state. On the basis of spectroscopic evidence, we therefore proposed that the so-called local ordered structure formed by physical aging can be ascribed to a kind of mesophase of PLLA. Of particular note, a very small amount of mesophase already exists in the initial state of melt-quenched PLLA sample, whereas it is totally undetectable in the melt-quenched poly(D,L-lactide) (PDLLA) sample. By temperature-dependent IR spectroscopy, it is found that the local ordered structure formed during the physical aging process will be "partially molten" rather than "totally molten" in the temperature region corresponding to the physical aging peak of aged PLLA. Such an observation can explain the phenomenon of physical aging enhanced cold crystallization rate.

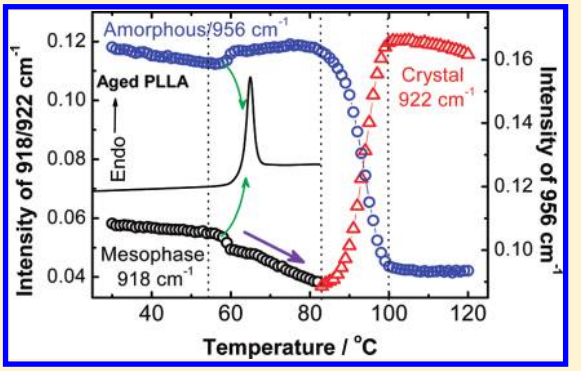

1. INTRODUCTION

Due to the nonequilibrium nature, the thermodynamic parameters (volume, enthalpy, etc.) and physical properties (density, permeability, etc.) of glassy polymer change continuously with time during annealing below the glass transition temperature.[1] Such processes are described as physical aging to distinguish it from chemical changes, such as oxidative degradation. Usually, segmental mobility or structural relaxation in a glassy polymer is thought to be associated with the changes in thermodynamic and mechanical properties that occur with physical aging. However, as a fundamental issue of polymer science, a complete understanding of physical aging remains a scientific challenge even though this topic has been investigated for more than half a century. Especially, the structural formation and evolutions that accompany physical aging of glassy polymer have not been clarified in detail.

Poly(L-lactic acid) (PLLA), one of the most popular *bioplastics* nowadays, has been chosen recently as a candidate to study the structural origin of physical aging by several groups.[2−7] For example, Pan et al.[6] concluded that the rearrangement from the high- to low-energy conformers, i.e., *gg* to *gt*, occurs with physical aging, while Na et al.[7] recently proposed that a local ordered structure with dense intermolecular packing, allowed by the coil−helix conformation transition, prevails in the aged glassy PLLA. We note that, in the past decades, the conformational adjustments and local ordered structures have been often used to describe the physical aging induced structural changes in other systems, such as poly(ethylene terephthalate) (PET)[8,9] and PMMA,[10,11] etc. Theoretically speaking, there is no question that the conformational adjustments of the local chain segmental and/or molecular group should be involved in the structural evolution with aging simply because they are the basic units for any other cooperatively structural changes, such as the coil−helix transition of the single chain driven by intrachain interaction or the chain packing induced by interchain interaction. However, due to the nature of "frozen" chain movement of the polymer at the temperature below the glass transition temperature (T_g), there are some questions on the so-called local ordered structure produced by physical aging. On one hand, it is still doubtful whether physical aging can induce the local ordered structure. On the other hand, there are some arguments on the nature of the so-called local ordered structure. For example, Qian et al.[9,12,13] used the concept of cohesional entanglement to describe the physical aging induced local ordered structure. They proposed that cohesional entanglement does not imply a kind of phase but a kind of binary or multiple interchain cohesion (attractive interaction) with local parallel alignment of neighboring chain segments. However, Hagege et al.[14] envisaged it as a mesomorphic phase of a nematic order, although the direct evidence has not been provided yet. Obviously, more efforts are required to understand the effect of physical aging on the structural formation in glassy polymer.

Fourier transform infrared spectroscopy (FTIR) is sensitive to both the local chemical and physical environment of polymer

Received: September 12, 2011
Revised: October 18, 2011
Published: October 18, 2011

chains, and it therefore has often been used to study the structural evolutions of polymer in various structural transitions, such as crystallization, melt, and even the subtle glass transition process.[15−19] However, it should be emphasized that accurate band assignments are the premise to correlate the relationship between spectra and physical structures. Yang and Hsu et al.[20−22] have performed spectroscopic simulation on various chain conformations and packing modes to fit their experimental spectra of PLLA for a time over ten years. Recently, Meaurio et al.[18,19] also contribute several important studies on spectral analysis of PLLA. In our previous works,[23−26] we have studied the various crystal modifications of PLLA and their crystallization processes in detail by using IR spectroscopy. These researches suggest that IR spectroscopy is a very useful tool to characterize the phase transition, crystal structure, and even the mesophase of PLLA. Therefore, on the basis of these solid works, the spectra−structure relationship of PLLA has been well established to some extent.

Usually, since the chain movement is restricted at the temperature region below T_g, the molecular reorganization from the nonequilibrium to equilibrium state during the physical aging of the quenched polymer is an extremely slow process. Moreover, the structural change during the physical aging process is very subtle. For these reasons, it has been thought that it is experimentally difficult to directly detect the structural evolutions of polymer during aging. In the present work, the structural evolutions during the isothermal physical aging process were in situ investigated by time-resolved FTIR, and the kinetics of structural formation are analyzed with a numerical data processor program for uniformly extracting the subtle spectral changes. Our results show that mesomorphic structure was developed in the physical aging process. By temperature-dependent IR spectroscopy, the thermal stability and the nature of this mesophase were further studied. It is expected that our observations will provide new insight to understand the local ordered structure of polymer obtained by physical aging.

2. EXPERIMENTAL SECTION

2.1. Material and Sample Preparation Procedure. PLLA (M_w = 1.1 × 10^5 g/mol, M_n = 4.5 × 10^4 g/mol) used in the present study was supplied from Mitsubishi Plastic Inc. Amorphous PLLA film was prepared by compression molding at 190 °C for 5 min at the molten state and subsequently quenched into ice water. The thickness of the melt-quenched film was ca. 40 μm.

2.2. Differential Scanning Calorimetry (DSC). DSC measurement was performed on a TA Q20 calorimeter system over a temperature range from 0 to 200 °C at a heating rate of 10 °C/min under a nitrogen gas flow at a rate of 50 mL/min.

2.3. FTIR Measurement and IR Data Treatment. FTIR spectra were measured with a Bruker TENSOR 27 spectrometer equipped with a DTGs detector. The normal transmission mode was employed for IR measurement. For in situ monitoring the structure changes of PLLA with aging via FTIR, the melt-quenched film was set on a Harrick variable-temperature cell, which was placed into a sample compartment of the spectrometer. The sample was then heated at 10 °C/min up to the aging temperature (below the T_g of PLLA) and annealed for 24 h. During the isothermal aging process, repeated measurement was taken every 10 min. After finishing the annealing, the aged sample was subsequently heated from 30 to 190 °C at 1 °C/min. During the heating process, FTIR spectra of the specimen were recorded at a 1 min interval. All the IR spectra of the specimen were collected by coadding 16 scans with 2 cm^{-1} resolution.

The intensity of IR bands was calculated automatically by a numerical data processor program for vibrational spectroscopy, Spina Version 3, which was developed by Yukiteru Katsumoto in the Ozaki Group of Kwansei-Gakuin University. Before the intensity calculation, all of the spectra were baseline corrected without smoothing. Then, peak heights were calculated at fixed wavenumber for all spectra by this program.

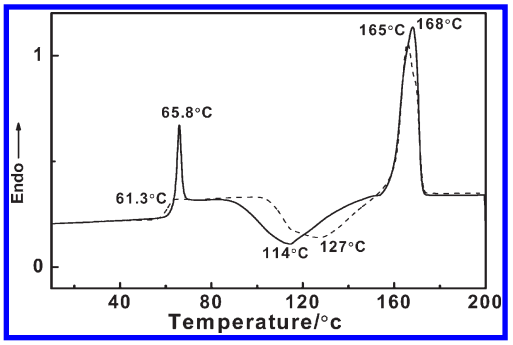

Figure 1. DSC curves of the PLLA samples unaged (dash) and aged at 51 °C for 24 h (solid) with a heating rate of 10 °C/min.

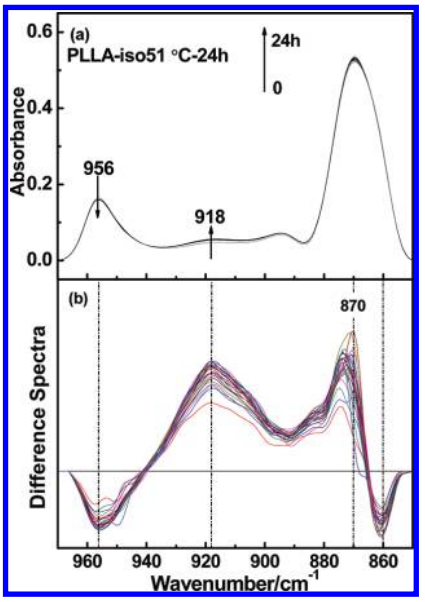

Figure 2. Time-resolved IR spectra (a) and difference spectra in the 970−850 cm^{-1} range (b) for PLLA aged at 51 °C for 24 h. These spectra were collected with a 1 h interval.

3. RESULTS AND DISCUSSION

3.1. Effect of Physical Aging on the Thermal Behavior of Melt-Quenched PLLA. PLLA is a semicrystalline polymer with a relatively low crystallization rate, and its amorphous sample with high transparency is often obtained by quenching it into ice water from the molten state. Figure 1 shows the DSC heating curves for such prepared samples without aging and that aged at 51 °C for 24 h. As denoted in these DSC curves, the T_g value of the unaged sample is around 61.3 °C, while it shifts to the higher temperature for an aged sample. Meanwhile, a so-called aging peak associated

with structural relaxation for the aged sample appears around 65.8 °C. Obviously, the cold crystallization rate for the aged sample is faster than that of the unaged one. Usually, structural relaxation due to isothermal physical aging near the glass transition in the glassy state gives rise to an endothermic peak in the vicinity of the glass transition region. Pan et al.[27] also found that the cold crystallization rate of PLLA is enhanced with aging. Therefore, our observation is consistent with the results in the literature.

Herein, the DSC data clearly suggest that physical aging has a prominent effect not only on the glass transition but also on the cold crystallization behavior of glassy PLLA. To understand these phenomena, it is necessary to study the microstructural evolution in glassy PLLA induced by physical aging. We therefore monitored the structural formation in the process of physical aging by time-resolved IR spectroscopy in the next section.

3.2. Structural Formation during the Physical Aging Process. Figure 2a shows the time-dependent spectral evolution in the chain backbone stretching region (970−850 cm^{-1}, assigned to skeletal C−C stretching coupled with CH_3 rocking modes[17,25]) during the physical aging process of melt-quenched PLLA at 51 °C for 24 h. It can be seen that there are very small spectral changes for these overlapped spectra. To make these spectral changes clearer, difference spectra as shown in Figure 2b were calculated by the subtraction of the initial spectrum from the spectra shown in Figure 2a. In the difference spectra, it clearly demonstrates that the intensity of the band at 918 cm^{-1} increases, while that of the band at 956 cm^{-1} decreases with aging time.

According to many spectroscopic studies on the polymorphism of PLLA, it has been found that the band at 956 cm^{-1} is ascribed to the amorphous phase, and the band around 920 cm^{-1} is related to the ordered helical chain conformation in various crystal modifications. For example, the bands at 923 and 908 cm^{-1} are the characteristic bands of 10/3 (α and α' form) and 3/1 (β form) helical chain conformation of PLLA, respectively. In our previous work,[21] by dealing with the phase transitions in melt-quenched PLLA−PEG−PLLA block copolymers, a band at 915 cm^{-1} is identified to be associated with the PLLA mesomorphic. Very recently, Stoclet et al.[28] studied the mesophase induced by tensile drawing from the amorphous state of PLLA with various techniques, including WAXD, DSC, and IR. They disclosed a band at 918 cm^{-1} that does not exist for either the amorphous or the crystalline phases and increases in parallel to the mesophase content of PLLA. Judging from these previous observations, the increase of the band at 918 cm^{-1} may indicate the growth of the mesomorphic structure in glassy PLLA. We will discuss this point later.

In the backbone stretching region of 970−850 cm^{-1}, the strongest band at 870 cm^{-1} is attributed to the C−C backbone stretching [ν(C−COO)]. In Figure 2a, a subtle increase of this band can be discernible. Such spectral changes are presented more clearly in the corresponding difference spectra as shown in Figure 2b. That is, a positive peak around 870 cm^{-1} in the difference spectra contributes its apparent increase of this band in the original spectra, while the negative peak at lower wavenumber (860 cm^{-1}) indicates that this band turns to sharper. In the cold crystallization process of PLLA, the band at 870 cm^{-1} shifts to higher wavenumber and becomes sharper. Na et al.[3] had proposed that this band is associated with the ordered structure of PLLA. Therefore, our spectral observation suggests that a local ordered structure, which is less ordered than the crystalline structure, does appear in the aging process.

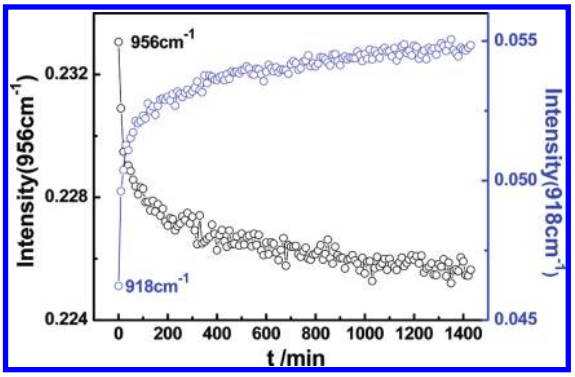

Figure 3. Intensity changes of the amorphous band at 956 cm^{-1} and the ordered band at 918 cm^{-1} of melt-quenched PLLA as a function of time during the physical aging process.

In Figure 3, the intensities of the bands at 918 and 956 cm^{-1} are plotted as a function of aging time. On the basis of the assignments above, the synchronous changes of the two bands suggest that there is a structural transition between the amorphous phase (956 cm^{-1} band) and the mesomorphic structure (918 cm^{-1} band) of PLLA.

Usually, the Kohlrausch−Williams−Watts (KWW) relaxation function, $\phi(t)$, was used to describe the dynamics of structural relaxation induced by physical aging. The kinetic process of approaching thermal equilibrium can be expressed as an exponential form as follows[29]

$$\phi(t) = \exp\left[-\left(\frac{t}{\tau}\right)^{\beta}\right] \quad (1)$$

where β (nonexponentiality parameter, $0 < \beta \leq 1$) represents the distribution of relaxation time and τ is the relaxation time. At a given aging temperature, if we assume the absorbance intensity of the band at 918 cm^{-1} is proportional to the amount of the amorphous phase in glassy PLLA, the structural relaxation function of the amorphous phase can be described by

$$\phi(t) = \frac{A_t - A_\infty}{A_0 - A_\infty} \quad (2)$$

where A_t is the peak intensity at the aging time t, and A_0 and A_∞ are the initial and final peak intensities in the whole aging process, respectively. By combining eqs 1 and 2, a new equation can be expressed in the following form

$$\ln\left[-\ln\left(\frac{A_t - A_\infty}{A_0 - A_\infty}\right)\right] = \beta \ln t - \beta \ln \tau \quad (3)$$

Of note, if we assume $n = \beta$ and $\ln k = -\beta \ln \tau$, this equation then turns to the Avrami plot as described in eq 4, which is often used for studying the crystallization dynamics.

$$\ln\left[-\ln\left(\frac{A_t - A_\infty}{A_0 - A_\infty}\right)\right] = n \ln t + \ln k \quad (4)$$

However, in the Avrami equation,[30] the physical meanings of the n and k are totally different from those of the β and τ in the KWW relaxation function. For describing the crystallization dynamics, k is the crystallization rate constant, and n is the Avrami exponent, which is related to the nature of nucleation and to the geometry of the growing crystals.[31]

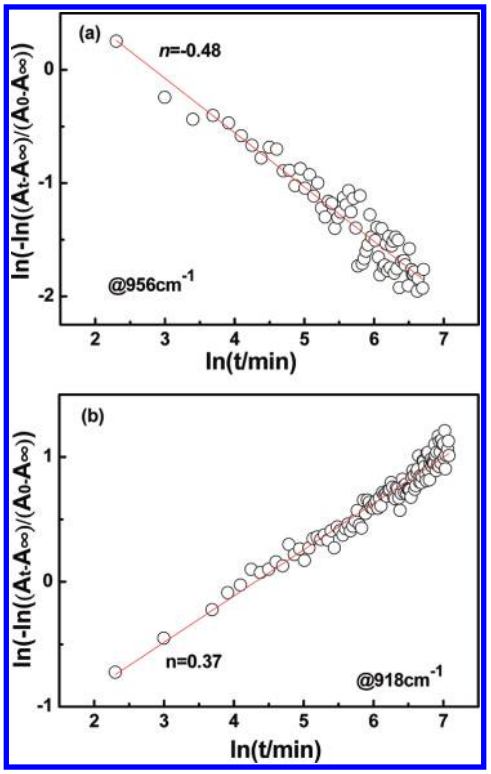

Figure 4. Curve-fitting results on (a) the structural relaxation of the amorphous phase (956 cm^{-1}) and (b) the growth of the mesomorphic phase (918 cm^{-1}) of the melt-quenched PLLA sample during the physical aging process.

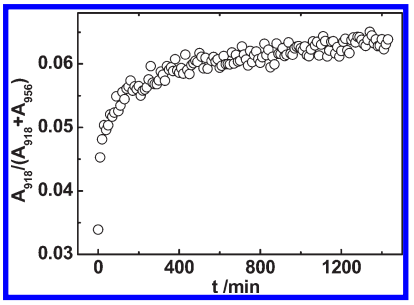

Figure 5. Evolution of the PLLA mesophase content as a function of aging time.

With eqs 3 and 4, the curve-fitting results on the structural relaxation of the amorphous phase and the growth of the mesomorphic phase were shown in Figures 4a and 4b, respectively. It is found that both β and n are around 0.4. The lower value of β for the glassy PLLA indicates the broader relaxation distribution which is consistent with other reports based on the calculation of enthalpy recovery value with DSC data. However, for the growth dynamic of the mesomorphic structure, $n \approx 0.4$ is far from the normal Avrami exponents (1−4) reported for the crystallization dynamics of polymer. This observation suggests that the formation dynamic of the local ordered structure, which is less ordered than that of a three-dimensional ordered crystal, is totally different from the crystallization process.

It should be pointed out that the evolution of the band at 918 cm^{-1} as a function of time does not satisfy the classical sigmoid curve predicted by the Avrami law. As show in Figure 5,

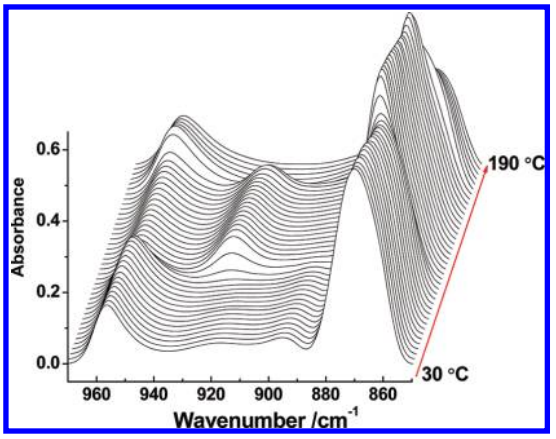

Figure 6. Spectral changes in the C−C backbone stretching vibration region during the heating process of the aged PLLA sample from 30 to 190 °C. The spectra were stacked every 5 °C.

it may be caused by the nonzero value of the mesophase content at the beginning of physical aging.

By considering that the decrease of the intensity at 956 cm^{-1} is synchronized with the increase of the intensity at 918 cm^{-1} during the physical aging process and both bands are well resolved, the quantitative assessment on the evolution of the mesophase content (X_{meso}) in whole material with aging time (t) is made with an approximate equation as follows

$$X_{meso}(t) = \frac{A_{918}}{A_{918} + A_{956}} \quad (5)$$

A_{918} and A_{956} are the intensities of the bands at 918 and 956 cm^{-1} at time t, respectively. The result is shown in Figure 5. It can be clearly seen that the mesophase exists in the initial amorphous sample, and the amount of physical aging induced mesophase is very limited ($\leq$3%). Usually, such limited mesophase in comparison with the actually amorphous part of the material is hard to detect by the WAXD technique. We will discuss the origin of the initial mesophase content later.

3.3. Melting of Physical Aging Induced Local Structure. To study the thermal stability of the mesomorphic structure as observed above, we performed the temperature-dependent IR measurement on the aged sample. As shown in Figure 6, in the heating process from 30 to 190 °C, the characteristic bands in the backbone stretching region of 970−850 cm^{-1} experience obviously changes due to the cold crystallization and melt of PLLA crystal as suggested by the DSC curve in Figure 1. However, the spectral change corresponding to the enthalpy recovery peak in the DSC data is hard to discern in the original spectral data. Therefore, the quantitative intensity changes of the characteristic bands at 918 and 956 cm^{-1} as a function of temperature are calculated and depicted in Figure 7a. In the temperature region from 30 to 190 °C, two abruptly synchronous exchanges of these two bands can be clearly revealed. One is located around the glass transition temperature (58 °C), and the other is located around the cold crystallization temperature region (90 °C).

Herein, it should be emphasized that the band at 922 cm^{-1} rather than the band at 918 cm^{-1} is associated with the crystallization process of PLLA. One may argue that they are so close that they are no different in nature. However, according to the previous discussion, we think that they are associated with the different ordered structures. That is, the band at 918 cm^{-1} is

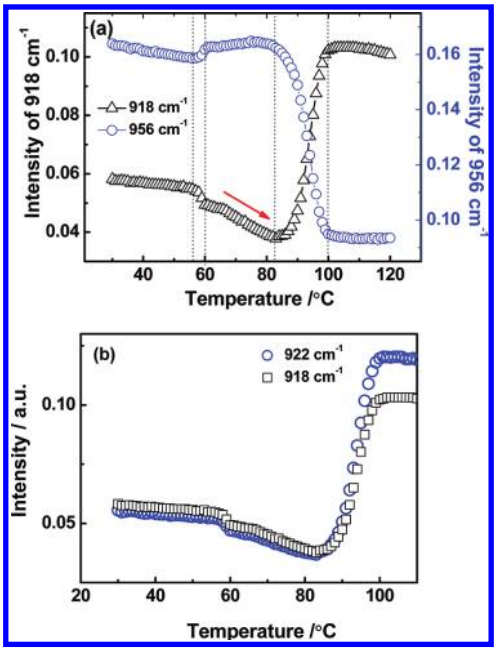

Figure 7. Intensity changes of the characteristic bands at 918 and 956 cm^{-1} as a function of temperature (a) and the intensity changes of the band at 918 cm^{-1} and the crystalline band at 922 cm^{-1} (b) during the heating processes of the PLLA sample aged at 51 °C for 24 h.

related to a kind of mesophase, whereas the band at 922 cm^{-1} is ascribed to the three-dimensional ordered crystal of PLLA. As shown in Figure 7b, the intensity changes of these two bands demonstrate similar trends with increasing temperature in the range of 30−110 °C. However, interesting enough, prior to the onset temperature (ca. 80 °C) for cold crystallization, the intensity of the band at 918 cm^{-1} is higher than that of the band at 922 cm^{-1}, which is totally in contrast to the trend in the temperature region of cold crystallization. This observation evidences that these two bands are dominantly in the temperature region of glass transition and the cold crystallization, respectively. Thus, the ordered structures characterized by the bands at 918 and 922 cm^{-1} are indeed different in nature, and they are associated with the mesophase and the crystal of PLLA, respectively. We will further clarify this point later.

On the basis of such assignment, the abrupt decrease of the 918 cm^{-1} band around 58 °C should indicate the "melting" of the mesophase that formed in the aging process, while the abrupt increase of the 922 cm^{-1} band is associated with the crystal growth of PLLA. As denoted by the red arrow in Figure 7a, it is found that the intensity of the band at 918 cm^{-1} decreases continuously prior to the cold crystallization temperature even after the abrupt "melting" behavior around 58 °C. This phenomenon suggests that the abrupt "melting" around 58 °C corresponding to the enthalpy recovery peak in the DSC curve is just a partial melting behavior, and the stabilities of the mesomorphic structures formed during the physical aging process have a wide distribution in the temperature region between the glass transition temperature and the onset temperature of cold crystallization. This observation may explain the origin of physical aging enhanced cold crystallization rate very well as demonstrated in Figure 1. For further clarifying this point, the temperature-dependent IR measurements were performed on both aged and unaged PLLA samples with a heating rate of 5 °C/min,

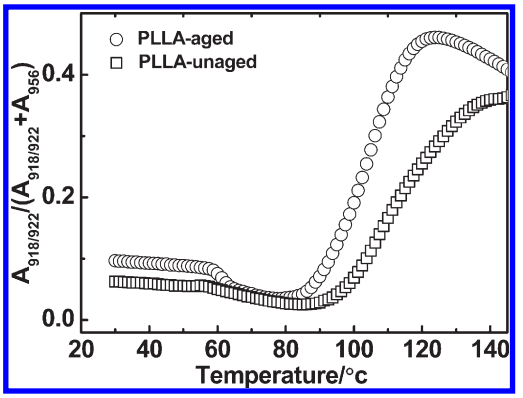

Figure 8. Evolutions of the relative content of the ordered phase as a function of temperature during the heating process of aged and unaged PLLA samples.

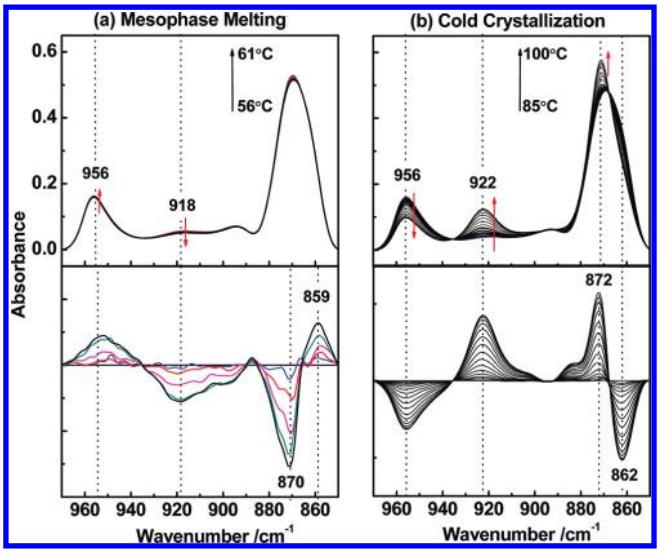

Figure 9. Temperature-dependent IR spectral changes (upper plane) and its difference spectra (bottom plane) for the melting process of the mesophase (a) and the cold crystallization process of the ordered crystal (b) during the heating process of the aged PLLA sample.

which is similar to the measurement condition of the DSC data shown in Figure 1. Meanwhile, the evolutions of the relative content of the ordered phases (local ordered mesophase and three-dimensional ordered crystal, $X_{meso/crystal}$) in the whole material as a function of temperature are calculated with the peak area of the amorphous band at 956 cm^{-1} (amorphous phase, A_{956}) and these ordered bands around 918/922 cm^{-1} ($A_{918/922}$). The equation is used as follows

$$X_{meso/crystal}(t) = \frac{A_{918/922}}{A_{918/922} + A_{956}} \quad (6)$$

As seen from the results shown in Figure 8, the mesophase content below the T_g for the aged sample is obviously higher than that in the unaged sample. Moreover, in contrast to the case for the aged sample, there is no "abrupt melting" around the glass transition temperature during the heating process for the unaged sample. With further heating above T_g, mesophase content for both samples decreases continuously prior to the cold crystallization temperature. However, the remaining mesophase has not

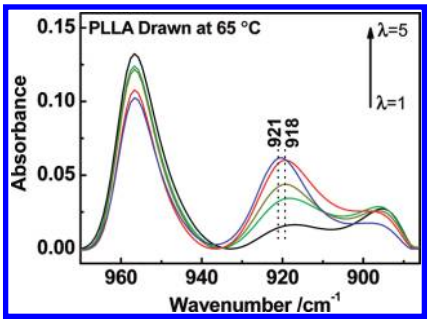

Figure 10. Unpolarized FTIR spectra of PLLA samples drawn at T_d = 65 °C with various draw ratios (λ).

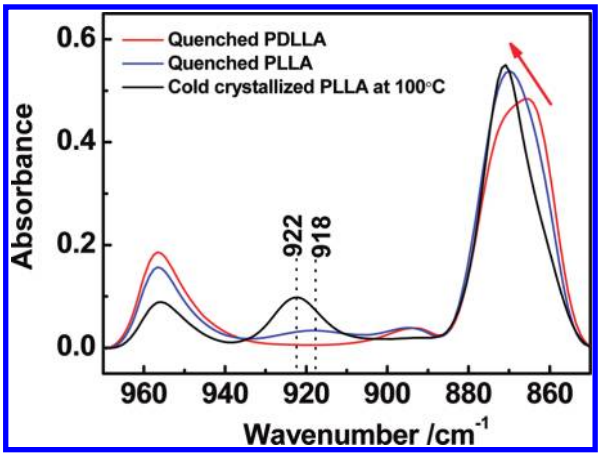

Figure 11. Detailed IR spectral variations in the spectral range of 870−830 cm^{-1} for four various samples.

decreased to zero value prior to the cold crystallization for the aged sample. These observations suggest that the partial molten mesophase accelerates the cold crystallization of the aged PLLA sample.

According to the quantitative analysis in Figure 7, the spectral evolutions for the abrupt melting process of the mesophase formed during the physical aging process and the cold crystallization process were separately displayed in Figures 9a and 9b. To enlarge the spectral changes, their difference spectra were also included for comparison. For both cases, the amorphous band at 956 cm^{-1} exists at the same peak position. However, the melting process of the mesophase and the cold crystallization process clearly demonstrates the changes of different characteristic bands, that is, 918/871 cm^{-1} for mesophase and 922/872 cm^{-1} for PLLA crystal, respectively. It should be pointed out that, in a recent Communication, Na et al.[4] also reported that, during the heating process of aged glassy PLLA, a sharp decrease in the absorbance of a crystalline sensitive band at 921 cm^{-1} occurs in both the glass transition region and melting process. They therefore proposed that a local ordered structure with dense intermolecular packing does prevail in the aged glassy PLLA. However, as revealed in the difference spectra of Figure 9a, it is found that the spectral change around T_g is located at 918 cm^{-1} rather than 921 cm^{-1}. The original spectral data again suggest that, corresponding to the enthalpy recovery peak around the glass transition temperature as shown in the DSC curve, there is a melting of the mesomorphic structure rather than a melting of the ordered crystal.

3.4. Nature of the Physical Aging Induced Local Ordered Structure of PLLA. Usually, the mesophase of the polymer can be obtained by uniaxially drawing of the amorphous polymer around the glass transition temperature or by fast cooling from the molten state. Stoclet et al.[24] studied the mesophase induced by tensile drawing from the amorphous state of a poly(D,L-lactide) (PDLLA) material containing 4 mol % of D-stereoisomer units, and they found that strain-induced occurrence of the mesophase as far as temperature did not exceed 70 °C. For further clarifying the suggested structure by the 918 cm^{-1} band as discussed above, we prepared the uniaxially oriented sample at 65 °C with our PLLA sample from the amorphous glassy state. As shown in Figure 10, with increasing the drawing ratio (DR), the IR spectra of the uniaxially oriented PLLA sample always demonstrate the 918 cm^{-1} band when the drawing ratio is below 4, while the characteristic 922 cm^{-1} band of the PLLA α/α' crystal occurs when the drawing ratio reaches 5. For the uniaxially oriented sample with low DR, our WAXD data show that the PLLA mesophase was obtained, which is consistent with Stoclet et al.'s conclusion.[24] Thus, the distinct 918 cm^{-1} band for the sample with low drawing ratio ($\leq$4) can be assigned to the characteristic band of the PLLA mesophase.

On the basis of this spectral evidence, it seems that local ordered structure obtained by the physical aging process has a similar structure with that of the PLLA mesophase produced by the uniaxial drawing method because they show the same 918 cm^{-1} band, which suggests that they have the same chain conformation. Usually, it is thought that the crystallization rate of the PLLA homopolymer is not so high that a totally amorphous rather than mesophase sample can be attained by the melt-quenched method. However, as displayed in the difference spectra of Figure 2, it is found that the characteristic 918 cm^{-1} band even appears at the beginning of the physical aging process. Therefore, we doubt that a very small amount of the PLLA mesophase can be also obtained by melt-quenched method. For examining this point, the IR spectra of the melting-quenched PLLA and PDLLA are compared in Figure 11. For comparison, the cold crystallized PLLA sample is also included. The PDLLA sample used here is totally amorphous because it contains 50 mol % of D-stereoisomer units. As shown in Figure 11, the 918 cm^{-1} band is clearly identified, while it totally disappears for the melt-quenched PDLLA sample. Meanwhile, it is found that the 918 cm^{-1} band for melt-quenched PLLA is very weak in intensity, and it is obviously different from the 921 cm^{-1} band for the cold crystallized sample. This evidence leads us to conclude that a small amount of mesomorphic structure of PLLA is already formed in the met-quenching process, and the physical aging below the glass transition temperature will enhance the amount of such mesophase to some extent.

4. CONCLUSION

In summary, the structural evolution of glassy PLLA during the isothermal physical aging process below the T_g was in situ monitored by FTIR spectroscopy. It is found that a mesomorphic structure already exists in the melt-quenched PLLA, and the physical aging below the glass transition temperature will enhance the amount of such mesophase. Our spectroscopic study shows that the mesophase developed in the aging process shows the same characteristic band at 918 cm^{-1} with that of the mesomorphic structure formed during the unaxially drawn process of PLLA from the glassy state. Because the band at 918 cm^{-1} is related to the C−C backbone vibration mode of PLLA, it is proposed that the PLLA chain conformation in such a mesophase is ordered to some extent

but less ordered than the regular 10/3 helix in the PLLA α crystal. By temperature-dependent IR spectroscopy, it is found that the mesomorphic structure formed during the physical aging process will be "partially molten" rather than "totally molten" in the temperature region corresponding to the physical aging peak of aged PLLA. This observation can explain the origin of the physical aging enhanced cold crystallization rate very well. Our results suggest that there is some structural similarity between the physical aging induced local ordered structure and the polymer mesophase obtained by uniaxial drawing of the amorphous sample or melt-quenched method.

AUTHOR INFORMATION

Corresponding Author

*Fax: +86-532-84022791. E-mail: zjm@qust.edu.cn (J.Z.); dyx@qust.edu.cn (Y.D.).

ACKNOWLEDGMENT

The financial support from the Natural Science Foundation of China (20804004 and 21174075), Taishan Mountain Scholar Constructive Engineering Foundation (TS20081120), and Natural Science Fund for Distinguished Young Scholars of Shandong Province (JQ200905) is greatly appreciated.

REFERENCES

(1) Chen, S. A.; Ni, J. M. *Macromolecules* **1992**, *25*, 6081–6089.
(2) Pan, P.; Zhu, B.; Inoue, Y. *Macromolecules* **2007**, *40*, 9664–9671.
(3) Aou, K.; Hsu, S. L.; Kleiner, L. W.; Tang, F. W. *J. Phys. Chem. B* **2007**, *111*, 12322–12327.
(4) Pyda, M.; Wunderlich, B *Macromolecules* **2005**, *38*, 10472–10479.
(5) Mano, J. F.; Ribelles, J. L .G.; Alves, N. M.; Sanchez, M. S. *Polymer* **2005**, *46*, 8258–8265.
(6) Pan, P. J.; Zhu, B.; Dong, T.; Yazawa, K.; Shimizu, T.; Tansho, M.; Inoue, Y. *J. Chem. Phys.* **2008**, *129*, 184902.
(7) Na, B.; Lv, R. H.; Zou, S. F.; Li, Z. J.; Tian, N. N. *Macromolecules* **2010**, *43*, 1702–1705.
(8) Wang, Y.; Shen, D. Y.; Qian, R. Y. *J. Polym. Sci., Part B: Polym. Phys.* **1998**, *36*, 783–788.
(9) Qian, R. Y.; Shen, D. Y.; Sun, F. G.; Wu, L. H. *Macromol. Chem. Phys.* **1996**, *197*, 1485–1493.
(10) Flory, A. L.; Ramanathan, T.; Brinson, L. C. *Macromolecules* **2010**, *43*, 4247–4252.
(11) Nam, J. E.; Lee, J. K.; Mauldin, T. C. *Polym. Bull.* **2010**, *65*, 825–835.
(12) Qian, R. Y.; Wu, L. H.; Shen, D. Y.; Napper, D. H.; Mann, R. A.; Sangster, D. F. *Macromolecules* **1993**, *26*, 2950–2953.
(13) Qian, R. Y. *Macromol. Symp.* **1997**, *124*, 15–26.
(14) Hagege, R. *Text. Res. J.* **1977**, *47*, 229–331.
(15) Pan, P. J.; Liang, Z. C.; Zhu, B.; Dong, T.; Inoue, Y. *Macromolecules* **2008**, *41*, 8011–8019.
(16) Krikorian, V.; Pochan, D. J. *Macromolecules* **2005**, *38*, 6520–6527.
(17) Kister, G.; Cassanas, G.; Vert, M. *Polymer* **1998**, *39*, 267–273.
(18) Meaurio, E.; López-Rodríguez, N.; Sarasua, J. R. *Macromolecules* **2006**, *39*, 9291–9301.
(19) Meaurio, E.; Zuza, E.; López-Rodríguez, N.; Sarasua, J. R. *J. Phys. Chem. B* **2006**, *110*, 5790–5800.
(20) Kang, S. H.; Hsu, S. L.; Stidham, H. D.; Smith, P. B.; Leugers, M. A.; Yang, X. Z. *Macromolecules* **2001**, *34*, 4542–4548.
(21) Yang, X. Z.; Kang, S. H.; Hsu, S. L.; Stidham, H. D.; Smith, P. B.; Leugers, A. *Macromolecules* **2001**, *34*, 5037–5041.
(22) Kalish, J. P.; Zeng, X. G.; Yang, X. Z.; Hsu, S. L. *Polymer* **2011**, *52*, 3431–3436.
(23) Zhang, J. M.; Tsuji, H.; Noda, I.; Ozaki, Y. *Macromolecules* **2004**, *37*, 6433–6439.
(24) Zhang, J. M.; Sato, H.; Furukawa, T.; Tsuji, H.; Noda, I.; Ozaki, Y. *J. Phys. Chem. B* **2006**, *110*, 24463–24471.
(25) Zhang, J. M.; Duan, Y. X.; Domb, A. J.; Ozaki, Y. *Macromolecules* **2010**, *43*, 4240–4246.
(26) Zhang, J. M.; Li, C. W.; Duan, Y. X.; Domb, A. J.; Ozaki, Y. *Vib. Spectrosc.* **2010**, *53*, 307–310.
(27) Pan, P. J.; Liang, Z. C.; Zhu, B.; Dong, T.; Inoue, Y. *Macromolecules* **2008**, *41*, 8011–8019.
(28) Stoclet, G.; Seguela, R.; Lefebvre, J. M.; Rochas, C. *Macromolecules* **2010**, *43*, 7228–7237.
(29) Williams, G.; Watts, D. C. *Trans. Faraday Soc.* **1970**, *66*, 80–85.
(30) Avrami, M. *J. Chem. Phys.* **1939**, *7*, 1103–1107.
(31) Hay, J. N. *Br. Polym. J.* **1971**, *3*, 74–79.